Available online at www.sciencedirect.com

SciVerse ScienceDirect

Journal of the European Ceramic Society 32 (2012) 3029–3034

www.elsevier.com/locate/jeurceramsoc

Short communication

Characteristics of the surface heat transfer coefficient for Al_2O_3 ceramic in water quench

Zhiliang Zhou [a], Fan Song [a,*], Yingfeng Shao [a], Songhe Meng [b], Chiping Jiang [c], Jia Li [d]

[a] State Key Laboratory of Nonlinear Mechanics (LNM), Institute of Mechanics, Chinese Academy of Sciences, Beijing 100190, China
[b] Centre for Composite Materials, Harbin Institute of Technology, Harbin 150080, China
[c] Solid Mechanics Research Center, Beijing University of Aeronautics and Astronautics, Beijing 100191, China
[d] LSPM CNRS UPR 3407, Université Paris 13, 93430 Villetaneuse, France

Received 3 August 2011; received in revised form 31 March 2012; accepted 15 April 2012
Available online 4 May 2012

Abstract

In this paper, we determined the surface heat transfer coefficient of Al_2O_3 ceramics quenched from different initial temperatures into a water bath at room temperature. By using the multipoint temperature measurement technique and the inverse heat conduction method, this coefficient was measured as function of surface temperature of the ceramics during the water quench. The obtained results indicate that the surface heat transfer coefficient largely depends not only on the initial quenching temperature and their evolution in quenching media but also on the sizes of tested specimens. In addition, brief discussion was completed on the rationality of the traditionally used approach, which considers the surface heat transfer coefficient as a joint constant of materials and quenching media, in previous studies on heat transfer and thermal stresses.

Keywords: Al_2O_3; Thermal shock resistance; Thermal properties; Surface heat transfer coefficient

1. Introduction

Thermal shock failure, which results in more than one-third of all failures of currently served ceramic components, heavily limits the applications of ceramic materials in thermal engineering.[1,2] However, the thermal shock failure mechanisms have not been understood very well up to now.[3–6] One of the most difficult problems is to determine the surface heat transfer coefficient (HTC) between the ceramics and the heat transfer media in the course of thermal shock, which plays a key role in deciding the thermal stresses generated in the materials.[7,8] The HTC between a material and a medium is traditionally considered to be a constant in the theories of heat transfer and thermal stresses.[5,9,10] However, it is currently proved that the HTC remarkably depends on the transient surface temperature of the tested specimens and the initial temperature of both the specimens and quenching media.[8,11] The errors on HTC may lead to considerable divergences between the theoretical and actual thermal stresses in predicting the thermal shock failure of ceramics.[5,9]

In existing studies, the HTC for ceramics in thermal shock was usually determined by measuring the critical temperature differences according to the theory of critical fracture stress.[4,8,11] Strictly speaking, the HTC obtained by this method only stands roughly for the effective values of the HTC during thermal shock at the critical temperature differences.[7,8] In addition, based on solving the inverse heat conduction problem, the variation of HTC as function of surface temperature of the tested specimens can be determined by measuring the temperature distribution in the specimens during thermal shock.[12–17] However, it is usually very difficult to measure accurately the evolution of the temperature field inside the ceramics. For example, an actual technological problem is how to effectively weld in the interior of the tested ceramic specimens thermocouples that have to work at high temperature environment. Therefore, this method has been applied widely to measure the HTC for metals and alloys, but rare is the case when it comes to ceramics.[17,18] Kim et al. applied this method to obtain the HTC of Al_2O_3 ceramics by assuming the specimens of small size to be the thermally lumped bodies during water quench.[7,18] However, this assumption is

* Corresponding author. Tel.: +86 10 8254 3961; fax: +86 10 8254 3935.
E-mail address: songf@lnm.imech.ac.cn (F. Song).

0955-2219/$ – see front matter © 2012 Elsevier Ltd. All rights reserved.
http://dx.doi.org/10.1016/j.jeurceramsoc.2012.04.027

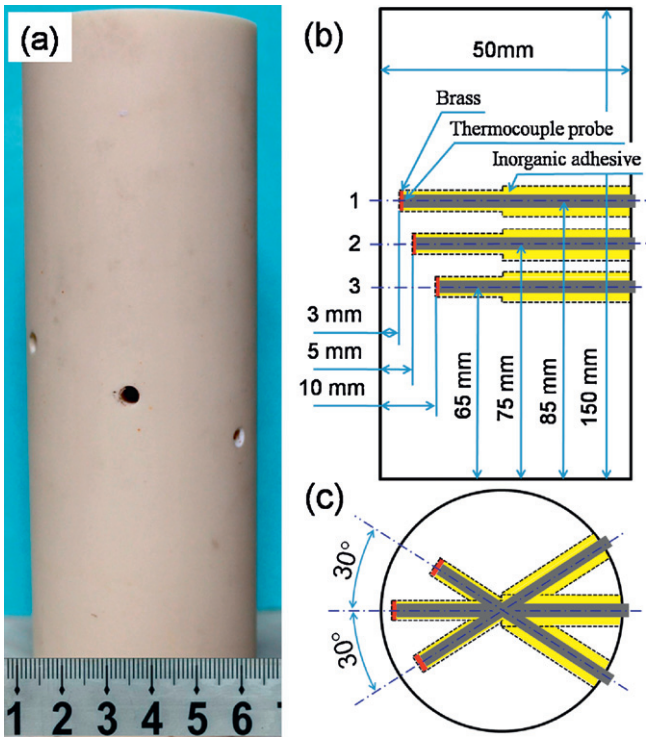

Fig. 1. Al_2O_3 specimen and the locations of thermocouples in the specimen.

not sufficient for the ceramics with lower thermal conductivity, because it ignores the thermal gradient effect that is directly responsible for the thermal stresses generated during thermal shock.[1,9]

In this study, firstly we experimentally measured the temperature field in Al_2O_3 specimens during water quench by implanting three thermocouples into the interior of each specimen at different depths. Then, the HTC of the specimens were obtained as function of their transient surface temperature during water quench by handling the measured temperature field and solving an inverse heat conduction problem. Finally, the properties and characteristics of the HTC are briefly discussed and compared with previous results.

2. Experimental procedure

2.1. Materials preparation and characterization

The ceramics used in the present study were made of Al_2O_3 powder (purity 99.5%, particle size 0.5 μm, Xiongdi material Co., Jiyuan, China) which was uniaxially pressed at 20 MPa into pellets and subsequently sintered in air at 1650 °C for 2 h without pressure. The specimens of the ceramics were cylindrical bars with the dimensions of 150 mm in height and 50 mm in diameter, as shown in Fig. 1(a).

The specimen surface was polished with SiC papers and diamond suspensions and then observed by a scanning electron microscopy (S-570, Hitachi, Tokyo, Japan). The morphology clearly displayed the random distribution of the pores on the surface, as shown in Fig. 2(a). After that, the microstructure at the surface that was thermally etched at 1500 °C for 0.5 h in air was also observed with the scanning electron microscopy, as shown in Fig. 2(b). Using the mean linear intercept method, the mean grain size at the surface was measured to be about 2.9 μm.

The bulk density of the specimens was measured to be $\rho = 3.85\ kg/m^3$ by the Archimedes technique, in which distilled water was used as the immersing medium. The relative density of the samples was readily computed to be about 96.7% by using the theoretical density of $3.98\ kg/m^3$ for Al_2O_3. The thermal diffusivity measurements were carried out on disk-shaped specimens at room temperature (about 20 °C) using a laser flash apparatus (Model 427, Netzsch).[19] The average thermal diffusivity of three tested specimens was $a = 5.4 \times 10^{-6}\ m^2/s$ and the experimental uncertainty was about ±5%. The heat capacity of alumina ceramic was taken as $C_p = 950\ J/kg\ K$.[20] Therefore, the thermal conductivity of the ceramic, $k = a\rho C_p$, was estimated to be about 20 W/m K.

In order to obtain the temperature fields in the interiors of the specimens during water quench, three blind shouldered-holes with identical diameter but different depths were perforated in each of the specimens by using a thin-wall diamond water drill bit (Hengxiang Super hard Material Co., Shangqiu, China). Firstly, three holes were drilled until the depth of a half of the specimen diameter by using a large drill bit (outer diameter 4.5 mm, wall thickness 0.4 mm), which were very helpful for

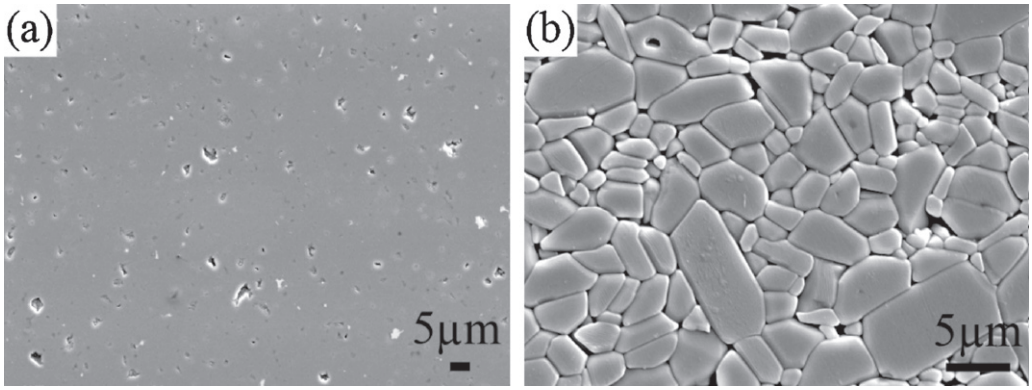

Fig. 2. SEM micrographs showing (a) the random distribution of pores on the ceramic surface and (b) the grain size on a surface of the ceramic. The mean grain size was measured by linear intercept technique to be about 2.9 μm.

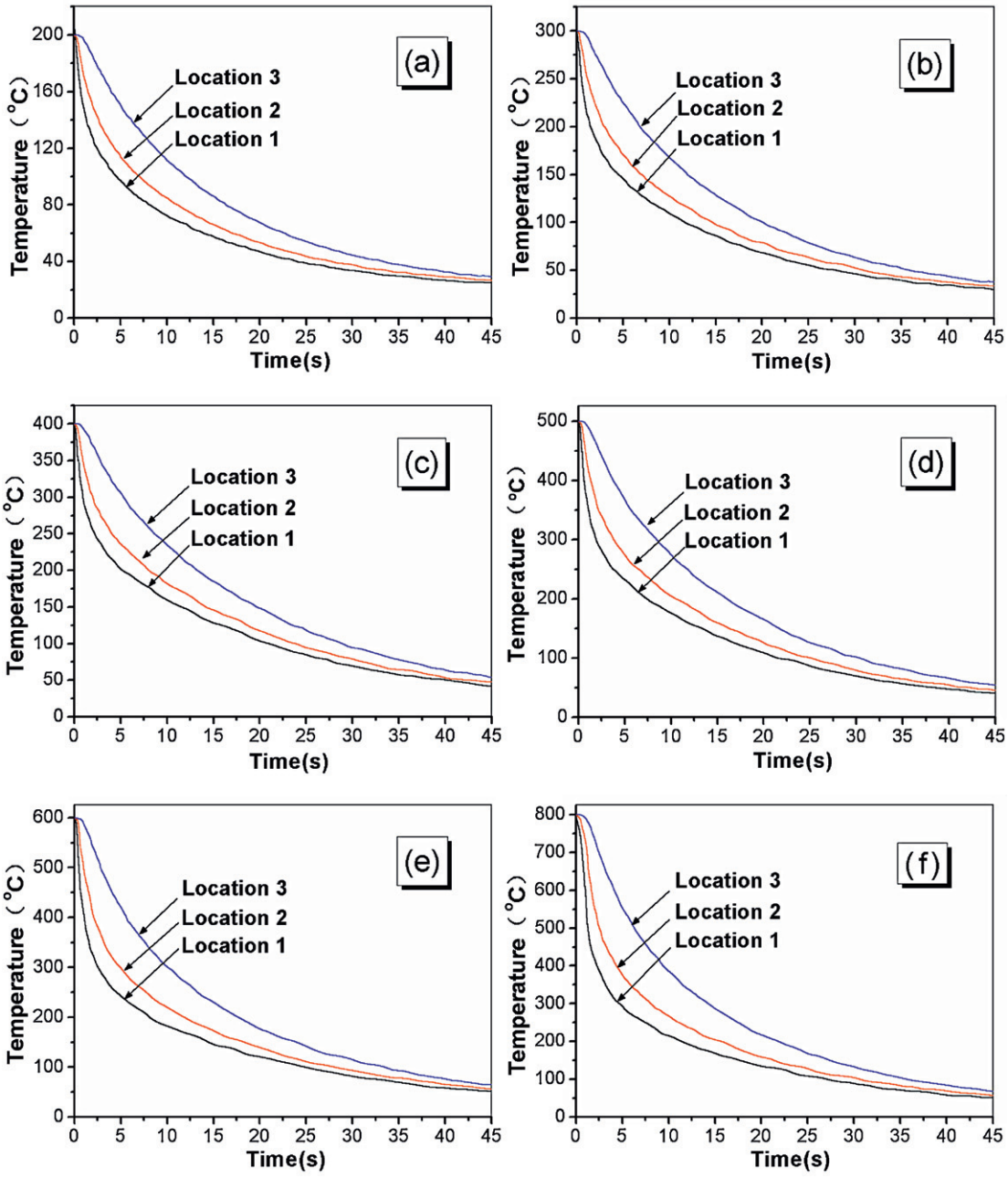

Fig. 3. Cooling curves for the initial quenching temperatures, T_0: (a) 200; (b) 300; (c) 400; (d) 500; (e) 600; (f) 800 °C.

future drilling of smaller and deeper holes. Then, these holes were further drilled by using a smaller drill bit (outer diameter 3.5 mm, wall thickness 0.35 mm) until the preset depths, as shown in Fig. 1(b) and (c). The rotate speed and feed rate of the bit were chosen as 1500 rpm and 0.05 mm/s, respectively. In such scenarios, collapse rarely happened on the walls and edges of the holes.

Because thermocouple probes could not be directly welded to the ceramics like metals, we used brass powder together with high-temperature inorganic adhesive to help fixing the thermocouples in the experiments. Firstly, small portion of compacted brass powder was placed into the bottom of the holes. Then, the armored K-type thermocouples with the diameter of 3 mm and a response time of 5 ms were separately inserted into the holes. The lacuna between the thermocouples and the holes was filled up with a high-temperature inorganic adhesive (Shuangjian DB5012, Shuangjian chemical Co., Ltd., Wuhan, China) to fix the thermocouples and to seal the holes, as shown in Fig. 1(b) and (c). After that, the thermocouple-fixed specimens were heated at a rate of 10 °C/min to about 920 °C (higher than the melting point of brass powder) and kept for 20 min in an electric furnace, so the thermocouple probes can be welded on the bottom of the holes with molten brass. After cooling to room temperature in the furnace, the other ends of the thermocouples were connected to a temperature acquisition system with an acquisition rate of 10 ksps.

We should note that the microcracks near the holes could be resulted from the process of drilling the holes, which could change the heat flow near the holes and promote the growth of cracks during thermal shock. However, the dimensions of the holes are much smaller than that of the specimens (3.5:50 in diameter) and the molten brass together with the inorganic adhesive that was filled up the lacuna can partly help to overcome the effects of the microcracks on the mechanical properties of the ceramic. So, the effects of the microcracks on both the heat flow near the holes and the growth of cracks during thermal shock become negligible. In addition, the thermal conductivity of the brass was much higher than that of the tested ceramic (about 8 times) and heat was transferred from the surface to the symmetrical axis of the cylindrical specimens in the experiments, as shown in Fig. 1. Therefore, the molten brass on the top of the thermocouple probe could hardly influence the heat transfer in the ceramic.

2.2. Water quenching test

The thermocouple-boned specimens were separately heated at a rate of 10 °C/min to six preselected temperatures and kept for 20 min in a vertical electric finance, where the preselected temperatures were 200, 300, 400, 500, 600 and 800 °C, respectively. Then, the heated specimens were quenched in a water bath of about 20 °C. The temperature fields and the cooling curves at the points where the thermocouples were placed were automatically recorded by the temperature acquisition system, as shown in Fig. 3.

In the quenching tests above, each of the specimens was used just one time at each of the preselected temperatures because of the thermal shock damage of the specimens. In general, the surface cracks would occur while the temperature difference between the heated specimens and the quenching media was greater than the critical temperature difference of the ceramics.[10,21,22]

3. Analysis of the inverse heat conduction

The ratio of the height and the diameter of the specimen is 3:1, and the positions of the three thermocouples can be roughly deemed to be in the middle of the specimen as shown in Fig. 1(b) and (c). The heat flows transferred from the two extremities of the ceramic cylinder can be ignored in the non-regular regime of heat transfer such as thermal shock.[23] Therefore, we approximately dealt with the heat conduction of each of the specimens in water quench as that of an infinite length cylinder, as shown in Fig. 4. The central axis of the cylinder was a symmetrical axis of the heat transfer, propagating from the surface to the interior. In the cylindrical coordinate system, the temperature field in the interior of the cylinder, $T(r, t)$, satisfies the heat conductive equation,

$$\frac{\partial T(r,t)}{\partial t} = a\left(\frac{\partial^2 T(r,t)}{\partial r^2} + \frac{\partial T(r,t)}{r\partial r}\right) \tag{1}$$

where $a = k/\rho C_p$ is the thermal diffusivity.

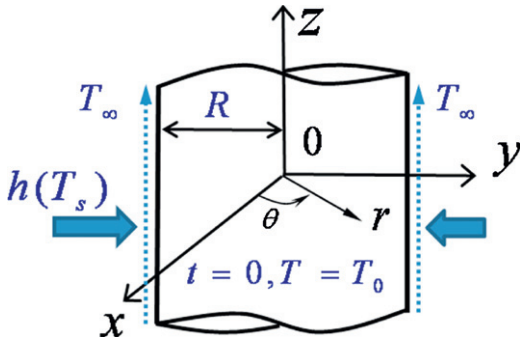

Fig. 4. An infinitely long cylinder suddenly exposed to a water bath at room temperature T_∞, in which the surface heat transfer coefficient of the materials, $h(T_s)$, was the function of the surface temperature, T_s.

Each of the cylinders was assumed to have a uniform initial temperature T_0, and its surface was suddenly exposed to a water bath of temperature T_∞ at initial time $t = 0$. So, the boundary and initial conditions of Eq. (1) can be written by

$$\begin{cases} \dfrac{-k(\partial T(r,t))}{\partial r} = q, & \text{at } r = R \\ \dfrac{\partial T(r,t)}{\partial r} = 0, & \text{at } r = 0 \\ T(r,0) = T_0 \end{cases} \tag{2}$$

where R is the radius of the cylinder, q is the heat flux entering the surface of the cylinder from the water bath during quench.

The surface heat flux over the Mth time interval $[t_{M-1}, t_M]$, q_M, is assumed to be constant. According to Beck's Sequential Function Specification method (SFS),[15] the sensitivity coefficient is defined as

$$X_M(r,t) = \frac{\partial T(r,t)}{\partial q_M} \tag{3}$$

It is used to describe the temperature distribution within a medium due to a step response in the surface heat flux.

Assuming there is a total of J thermocouples ($J = 3$ here), at the time t_M and location r_p ($p = 1, 2, \ldots, J$), the measured temperature is represented by $Y_{p,M}$, the computed temperature using Eqs. (1) and (2) is represented by $T_{p,M}(q_M)$. According to the SFS method, the least squares error is defined as

$$S = \sum_{P=1}^{J} [Y_{P,M} - T_{P,M}(q_M)]^2 \tag{4}$$

Differentiating Eq. (4) with respect to q_M, gives:

$$\frac{\partial S}{\partial q_M} = 2\sum_{P=1}^{J} [Y_{P,M} - T_{P,M}(q_M)] X_{P,M}(q_M) = 0 \tag{5}$$

where $X_{P,M}(q_M) = (\partial T_{P,M}(q_M))/(\partial q_M)$

In addition, $T_{p,M}(q_M)$ can be expanded into a Taylor series with respect to the surface heat flux q^*

$$T_{P,M}(q_M) = T_{P,M}(q^*) + (q_M - q^*) X_{P,M}(q^*) + \cdots \tag{6}$$

Table 1
The maximum surface heat transfer coefficient h_{max} and the mean surface heat transfer coefficient $\bar{h}$ for different initial quenching temperatures T_0.

T_0 (°C)	200	300	400	500	600	800	a.v. ± s.d.
h_{max} (10^4 W/m^2 K)	1.49	1.64	1.91	2.59	2.83	2.93	2.23 ± 0.63
$\bar{h}$ (10^4 W/m^2 K)	0.87	0.89	0.93	1.11	1.23	1.05	1.01 ± 0.14

where

$$X_{P,M}(q^*) = \frac{\partial T_{P,M}(q_M)}{\partial q_M}\Big|_{q_M = q^*}.$$

The higher-order derivatives are zero. Moreover, $X_{p,M}(q_M)$ does not depend on q_M for the linear case of temperature independent thermal properties.[15] Consequently we have $X_{p,M}(q_M) = X_{p,M}(q^*)$.

Substituting Eq. (6) into Eq. (5) gives:

$$q_M = \frac{q^* + \left\{\sum_{P=1}^{J} X_{P,M}(q^*)[Y_{P,M} - T_{P,M}(q^*)]\right\}}{\sum_{P=1}^{J} X_{P,M}^2(q^*)} \quad (7)$$

Firstly, an arbitrary q^* was chosen in Eq. (7), then the surface heat flux q_M in the time interval $[t_{M-1}, t_M]$ can be obtained by iterative computation. Once the surface heat flux is obtained, the transient surface temperature $T_{s,M}$ at time t_M can be determined by Eqs. (1) and (2). Then the heat transfer coefficient in this time interval can be determined by Newton's law of cooling,

$$h_M = \frac{q_M}{T_{s,M} - T_\infty} \quad (8)$$

Therefore, $h(T_s)$ can be readily figured out as a function of the surface temperature T_s of the cylinder.

4. Results and discussion

The Al_2O_3 ceramic specimens were quenched into a room temperature water bath from different initial temperatures (T_0 = 200, 300, 400, 500, 600 and 800 °C, respectively). The HTC was obtained as function of surface temperature of the specimens in the course of water quench, as shown in Fig. 5. We found that the HTC curve $h(T_s)$ was strongly dependent not only on the variation of the surface temperature during water quench but also on the initial quenching temperature T_0. However, all the HTC curves shared a similar shape in the course of water quench. Each of the $h(T_s)$ curves exhibits a maximum value h_{max} that increases monotonically with the increase of the initial quenching temperature. In addition, the average value of h_{max} corresponding to all initial quenching temperatures was readily calculated to be about $(2.23 \pm 0.63) \times 10^4$ W/m^2 K (a.v. ± s.d.), which changes by about 28% relative to all of h_{max}, as listed in Table 1.

Further, the mean value of each of the HTC curves was defined to be

$$\bar{h} = \frac{1}{T_0 - T_\infty} \int_{T_\infty}^{T_0} h(T_s) dT_s \quad (9)$$

and $\bar{h}$ corresponding separately to each of the $h(T_s)$ curves was computed, as listed in Table 1. Unlike h_{max}, the mean HTC $\bar{h}$ does not increase monotonically as the initial quenching temperature increases. It was figured out that the maximum value of $\bar{h}$ should occur in the vicinity of T_0 = 600 °C. Also, we could calculate the average value of $\bar{h}$ to be $(1.01 \pm 0.14) \times 10^4$ W/m^2 K, which changes by less than 14% relative to all of $\bar{h}$. This result indicates that traditionally applying the HTC as a constant, for example, the average value of HTC, is roughly reasonable during the steady heat conduction of materials, whereas, results in a certain error during the unsteady heat conduction, especially in the thermal shock of ceramics.

We compared the results obtained here with the results in previous studies. On the one hand, Kim et al.[7] used the method similar to the present study to investigate the Al_2O_3 ceramic plates with characteristic size of 1 mm. The obtained maximum HTC is of about 6.0×10^4 W/m^2 K under the initial temperatures ranging from 270 to 370 °C. This value is slightly larger than the maximum value that obtained above in the same temperature range. This difference is essentially induced by the fact that the characteristic size of specimens in the present experiments is much greater than that used in Kim et al. In fact, it had been proved that there exist remarkable size and boundary effects of specimens in quenching experiments: the larger is the specimen size, the smaller is the value of the HTC.[8–10] On the other hand, Singh et al.[8] by measuring the critical temperature differences of Al_2O_3 cylindrical specimens with the diameters of 3.18–9.53 mm in water quench, obtained the effective HTC values ranging from 0.65 to 4.43×10^4 W/m^2 K. In addition, other researchers also displayed the similar results to the present study.[16,17] As stated above, our results are in very good agreement with the results obtained in previous studies.

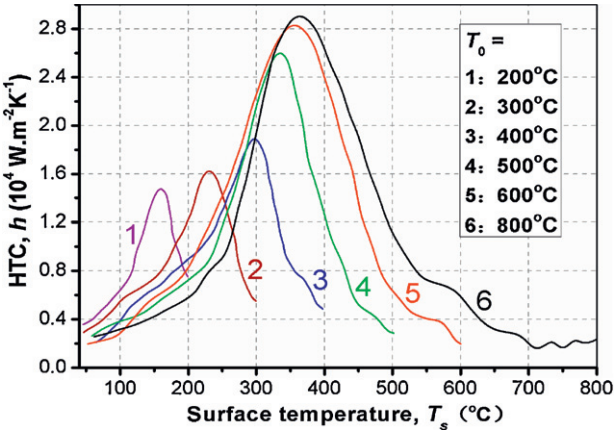

Fig. 5. Surface heat transfer coefficients (HTC) for Al_2O_3 ceramic bars quenched into the room temperature water bath from different initial temperatures T_0 are shown as the functions of the transient surface temperatures of the specimens.

5. Conclusions

The surface heat transfer coefficient of Al_2O_3 ceramics in water quench, which is remarkably dependent on the initial temperature and the surface temperature of the specimens, are determined as function of the transient surface temperature during quenching tests. Because the mean values of the surface heat transfer coefficient only vary slightly, it is reasonable to consider the surface heat transfer coefficient of the ceramic as a constant during steady heat transfer. However, using constant value of the surface heat transfer coefficient may introduce a certain error in unsteady heat transfer, especially in the course of thermal shock. In addition, the variation of the surface heat transfer coefficient is also influenced by the size effect of the tested specimens.

Acknowledgments

This work was supported by the National Natural Science Foundations of China (Grants 11061130550, 11072252, 91016029, 11102208 and 11021262) and the Inst. Mech. Innovation Program. Jia Li gratefully acknowledges the funding of the French ANR program T-Shock OTP J11R087.

References

1. Kingery WD. Factors affecting thermal stress resistance of ceramic materials. *J Am Ceram Soc* 1955;**38**(1):3–15.
2. Danzer R, Lube T, Supancic P, Damani R. Fracture of ceramics. *Adv Eng Mater* 2008;**10**(4):275–98.
3. Pompe WE. Thermal shock behavior of ceramic materials-modelling and measurement. In: Schneider GA, Petzow G, editors. *Thermal shock and thermal fatigue behavior of advanced ceramics*. Netherlands: Kluwer Academic Publishers; 1993. p. 3–14.
4. Absi J, Glandus JC. Improved method for severe thermal shocks testing of ceramics by water quenching. *J Eur Ceram Soc* 2004;**24**(9):2835–8.
5. Davidge RW, Tappin G. Thermal shock and fracture in ceramics. *Trans Br Ceram Soc* 1967;**66**(8):405–22.
6. Song F, Meng SH, Xu XH, Shao YF. Enhanced thermal shock resistance of ceramics through biomimetically inspired nanofins. *Phys Rev Lett* 2010;**104**(12):125502.
7. Kim Y, Lee WJ, Case ED. The measurement of the surface heat transfer coefficient for ceramics quenched into a water bath. *Mater Sci Eng A* 1991;**145**(1):L7–11.
8. Singh JP, Tree Y, Hasselman DPH. Effect of bath and specimen temperature on the thermal stress resistance of brittle ceramics subjected to thermal quenching. *J Mater Sci* 1981;**16**(8):2109–18.
9. Hasselman DPH. Strength behavior of polycrystalline aluminum subjected to thermal shock. *J Am Ceram Soc* 1970;**53**(9):490–5.
10. Sherman D, Schlumm D. Thickness effect in thermal shock of alumina ceramics. *Scr Mater* 2000;**42**(8):819–25.
11. Becher PF. Effect of water bath temperature on the thermal shock of Al_2O_3. *J Am Ceram Soc* 1981;**64**(1):C17–8.
12. Su J, Hewitt GF. Inverse heat conduction problem of estimating time-varying heat transfer coefficient. *Numer Heat Transfer A: Appl* 2004;**45**(8):777–89.
13. Hwang JJ, Hwang GJ, Yeh RH, Chao CH. Measurement of interstitial convective heat transfer and frictional drag for flow across metal foams. *J Heat Transfer: Trans ASME* 2002;**124**(1):120–9.
14. Chantasiriwan S. Inverse heat conduction problem of determining time-dependent heat transfer coefficient. *Int J Heat Mass Transfer* 1999;**42**(23):4275–85.
15. Beck JV, Blackwell B, Clair Jr CRS. *Inverse heat conduction: ill-posed problems*. New York: Wiley; 1985.
16. Hachisu T, Sakai T, Taguchi T. Transient temperature distribution in circular cylinder during quenching. *Heat Transfer: Jpn Res* 1981;**10**(1):52–64.
17. Lanin AG, Tkachev AL. Numerical method of thermal shock resistance estimation by quenching of samples in water. *J Mater Sci* 2000;**35**(9):2353–9.
18. Lee WJ, Kim Y, Case ED. The effect of quenching media on the heat transfer coefficient of polycrystalline alumina. *J Mater Sci* 1993;**28**(8):2079–83.
19. Liu ZG, Ouyang JH, Zhou Y, Li YJ, Xia XL. Densification, structure, and thermophysical properties of ytterbium–gadolinium zirconate ceramics. *Int J Appl Ceram Technol* 2009;**6**(4):485–91.
20. Kubaschewsji O, Alcock CB, Spencer PJ. *Materials thermochemistry*. 6th ed. Oxford: Pergamon Press; 1993. p. 257–323.
21. Becher PF, Lewis D, Carman KR, Gonzalez AC. Thermal shock resistance of ceramics – size and geometry effects in quench tests. *Am Ceram Soc Bull* 1980;**59**(5):542–8.
22. Shao YF, Xu XH, Meng SH, Bai GH, Jiang CP, Song F. Crack patterns in ceramic plates after quenching. *J Am Ceram Soc* 2010;**93**(10):3006–8.
23. Carslaw HS, Jaeger JC. *Conduction of heat in solids*. 2nd ed. Oxford: Clarendon Press; 1959.